Journal of Marine Research, 69, 137–165, 2011

Transport and retention of the mitten crab (*Eriocheir sinensis*) in a Mid-Atlantic estuary: Predictions from a larval transport model

by Charles E. Tilburg[1], Ana I. Dittel[2], Douglas C. Miller[2] and Charles E. Epifanio[2]

ABSTRACT

Invasive species cause extensive ecological damage in freshwater and marine habitats and are a threat to biodiversity in aquatic ecosystems world-wide. One such species, the Chinese mitten crab, *Eriocheir sinensis,* has invasive populations in northern Europe and San Francisco Bay, and there are confirmed reports of breeding female crabs in both the Chesapeake and Delaware Bays. Despite their threat to these ecosystems, there are still large gaps in the current understanding of this species' larval biology that are critical to predicting the potential for large populations to establish in East Coast bays and estuaries. We addressed these issues by using a physical circulation model of Delaware Bay and the adjacent coastal ocean coupled to a modified particle advection scheme. We used this model to examine the effects of different physical mechanisms and larval behavior on transport, retention, and settlement of larvae in the bay. The circulation model produced flow fields using observed winds and river discharge for 2006 as well as systematic variations of river discharge and wind direction. Since little is known regarding mitten crab larval behavior, the larval component was purposefully general and incorporated a suite of behaviors such as tidal, diel, and ontogenetic vertical migration; however, results of this study showed that vertical migration affects the magnitude, but not locations of larval settlement. Simulations revealed that changes in the time and location of spawning can result in large variations in retention and settlement of larvae in Delaware Bay and the coastal ocean, due to seasonal variations of the physical flow field. Overall results of our study showed that the estuarine and coastal circulation typically found along the Middle Atlantic coast of the United States can result in significant retention of new and established *E. sinensis* populations in large estuaries as well as transport of larvae to new coastal locations.

1. Introduction

Invasive species cause extensive ecological damage in freshwater and marine habitats and are a threat to biodiversity in aquatic ecosystems worldwide (Pimentel *et al.,* 2000; Bax *et al.,* 2001; Sorte *et al.,* 2010). Traits that contribute to success of invasive aquatic species include high fecundity, wide tolerance to environmental factors, and life-history stages that disperse over long distances (Ruiz *et al.,* 2000; Lodge *et al.,* 2006). These

1. Department of Marine Sciences, University of New England, Biddeford, Maine, 04005, U.S.A. ***email: ctilburg@une.edu***

2. College of Earth, Ocean and Enviornment, University of Delaware, Lewes, Delaware, 19958, U.S.A.

characteristics are particularly evident among brachyuran crab species where females often produce $>10^4$ eggs per year, adults and juveniles are tolerant of broad variation in salinity and temperature, and larval forms can disperse hundreds of km from a spawning site (Carlton and Cohen, 2003).

The life history of brachyuran crabs involves courtship, copulation, internal storage of sperm, and external brooding of fertilized eggs (Epifanio, 2007). Larval development includes a number of zoeal stages and a single megalopal stage. The larvae are usually planktonic and maintain position in the water column through active swimming. Swimming speed increases as larvae pass through the various stages, and velocities range from a few mm s^{-1} to a few cm s^{-1} (Forward, 1990; Luckenbach and Orth, 1992; Epifanio *et al.,* 1999). These swimming speeds are considerably slower than ambient currents in estuarine or coastal environments (Garvine, 1991). Accordingly, the larval forms of brachyurans cannot influence their dispersal by horizontal swimming. However, swimming in the vertical plane allows larvae to take advantage of vertical shear in current velocities with attendant consequences for horizontal transport (Epifanio and Garvine, 2001; DiBacco *et al.,* 2001). This type of swimming behavior is particularly important in estuarine habitats where vertical migration at tidal frequency results in rapid landward or seaward transport of larvae, depending on whether migration is in phase with ebb- or flood-tidal flow (Forward and Tankersley, 2001; Forward *et al.,* 2003, 2007).

The majority of brachyuran crab species occur in estuarine or coastal-ocean habitats, but some species spend at least part of their lives in freshwater or on land (Williams, 1984). A number of coastal and estuarine crab species are bioinvasive and have wide distribution beyond their native range. These include the green crab *Carcinus maenas,* the Asian shore crab *Hemigrapsus sanguineus,* and the Chinese mitten crab *Eriocheir sinensis.* Each of these species is multi-continental in distribution, and wide expanses of open ocean separate invasive populations from native stock. For example, *E. sinensis* occupies a number of widely separated habitats outside its native range along the east coast of Asia (see review by Dittel and Epifanio, 2009). Invasive populations have existed in northern Europe since the early 20th century (Panning, 1939), and more recently a breeding population has become established in the San Francisco Bay system along the west coast of North America (Rudnick *et al.,* 2000). Ballast water is the most probable vector for both invasions (see review by Dittel and Epifanio, 2009).

E. sinensis spends most of its adult phase in freshwater habitat (Jin *et al.,* 2001). In their native range, mitten crabs migrate downstream to higher salinity areas to mate in late fall and winter (Jin *et al.,* 2001, 2002; Zhang *et al.,* 2001). Downstream migration begins once females have gone through the puberty molt. Investigations in San Francisco Bay have described similar patterns of migration and mating (Veldhuizen, 1998; Rudnick *et al.,* 2000, 2003). Adults in both native and invasive populations make a single reproductive migration and die after the spawning season is over (Kobayashi and Matsuura, 1995a,b). Spawning age can vary between 2 to 5 years (Dittel and Epifanio, 2009). Female mitten crabs are highly fecund, and each female may produce 3 or more broods during the

reproductive season (Panning, 1939). A typical brood contains between 10^5 and 10^6 eggs (Panning, 1939; Cohen and Carlton, 1995).

Zoeae in native populations appear in early spring, and megalopae are first seen in May and June (Zhao, 1980; Jin *et al.,* 2002). The reproductive season typically extends through the summer (see review by Dittel and Epifanio, 2009). Development consists of five zoeal stages and a megalopal stage (Kim and Hwang, 1995; Montu *et al.,* 1996). Larval duration varies from several weeks to almost 3 months (85 days) depending on water temperature, which in native habitats ranges from 12°C to 20°C during the spawning season (Anger, 1991; Dittel and Epifanio, 2009). There has been little study of the spatial distribution of larvae in native or invasive habitat, and there have been no laboratory studies of larval swimming behavior (Dittel and Epifanio, 2009).

Chinese mitten crabs have recently appeared in the Chesapeake and Delaware bays on the east coast of North America, and there are reports of breeding females in both estuaries (Ruiz *et al.,* 2006). The potential for large populations of mitten crabs in these bays has not been determined, but invasive populations of *C. maenas* and *H. sanguineus* are well established on the east coast of North America, and each has had negative effects on native crab species (Grosholz *et al.,* 2000; Jensen *et al.,* 2002; Lohrer and Whitlatch, 2002; MacDonald *et al.,* 2007). Invasive populations of mitten crabs have caused hundreds of millions of dollars in economic and ecological damage (see review by Dittel and Epifanio, 2009). Economic impacts center largely on the burrowing activity of the crabs which damages stream banks and levees, and the annual spawning migration which interferes with fishing activities and irrigation projects.

In this paper, we test the hypothesis that estuarine and coastal circulation will result in the retention of recently established invasive *E. sinensis* populations along the Middle Atlantic coast of the United States. Our study focuses on Delaware Bay and the adjacent coastal ocean. Our methodology employs modeling techniques that allow simulation of larval transport under a variety of scenarios that include: (1) different spawning dates and locations; (2) different wind and outflow conditions; and (3) different patterns of larval swimming behavior. These modeling techniques have allowed us to investigate the details of larval transport in native species in this region and provide a powerful tool for assessing the potential for dispersal of invasive species as well (Petrone *et al.,* 2005; Tilburg *et al.,* 2005, 2006, 2007a, 2008, 2009).

While these previous model studies have provided detailed information on both dispersal and settlement of larvae in Delaware Bay, they examined the fate of blue crabs (*Callinectes sapidus*) and fiddler crab (*Uca pugnax*) larvae, which may differ from mitten crabs in both the timing of spawning and vertical migratory behavior. In native Asian habitats, mitten crabs spawn in early spring (Dittel and Epifanio, 2009), while the spawning season for blue crabs and fiddler crabs (as well as the invasive Asian shore and green crabs) in Delaware Bay extends from early summer through early fall (Dittel and Epifanio, 1982). Accordingly, mitten crab larvae in large-river estuaries like Delaware Bay are likely to be influenced by high-flow events (see below), while the two native (and the

current invasive) species are not. Moreover, the vertical distributions of both blue crab larvae and fiddler crab larvae are well known (Epifanio, 2007; Epifanio *et al.,* 1988) and have been incorporated into previous modeling efforts. In contrast, there is nothing known about the vertical distribution of mitten crab larvae (Dittel and Epifanio, 2009), and the modeling exercises in the present paper investigate a number of plausible scenarios.

2. Materials and methods

a. Study site

Delaware Bay is a partially mixed estuary that exhibits weak stratification during the summer months (Garvine, 1991; Wong and Münchow, 1995). In the absence of strong winds, buoyancy-driven flow exits the bay along the southern shore and continues southward along the inner continental shelf as the Delaware Coastal Current (Münchow and Garvine, 1993). Winds can modify this buoyancy-driven flow, both alongshelf (e.g. Tilburg *et al.,* 2007b) and along-estuary (e.g. Janzen and Wong, 2002). Tides, river discharge, and coastal winds are the main agents controlling transport of surface-dwelling larval forms in the region (Epifanio, 1995; Epifanio and Garvine, 2001; Natunewicz *et al.,* 2001).

b. Circulation model

A coupled numerical model simulated both the physical dynamics within the study area and the presumed behavior of *E. sinensis* larvae. The model was used to determine the effectiveness of physical mechanisms and larval behaviors in the retention of larvae in Delaware Bay. The model was based on a particle advection scheme coupled to a hydrodynamic circulation model that was previously used in a number of larval transport studies of the region (e.g. Tilburg *et al.,* 2005, 2006, 2007a). The circulation model used in this study was ECOM3d, which is a validated, primitive-equation, finite-difference model that includes tidal variations, wind forcing, variable river discharge, and vertical structure of the velocity fields. This model and the similar Princeton Ocean Model have been used extensively to study transport on continental shelves (e.g., Kourafalou *et al.,* 1996; Whitney and Garvine, 2006). Whitney and Garvine (2006) detail an extensive comparison of output from the circulation model with observations from an estuarine salinity climatology, freshwater delivery to the shelf, salinity mappings, and surface drifter data. Consequently, the model is only briefly described here and the interested reader is referred to Whitney and Garvine (2006) for a more comprehensive description of the model.

The model domain includes Delaware Bay, a portion of the Delaware River, and the adjoining coastal region (Fig. 1). The model equations on a (x, y, z) cartesian coordinate system are described by Kourafalou *et al.* (1996) and shown here:

$$\nabla \mathbf{u} + \frac{\partial w}{\partial z} = 0 \tag{1}$$

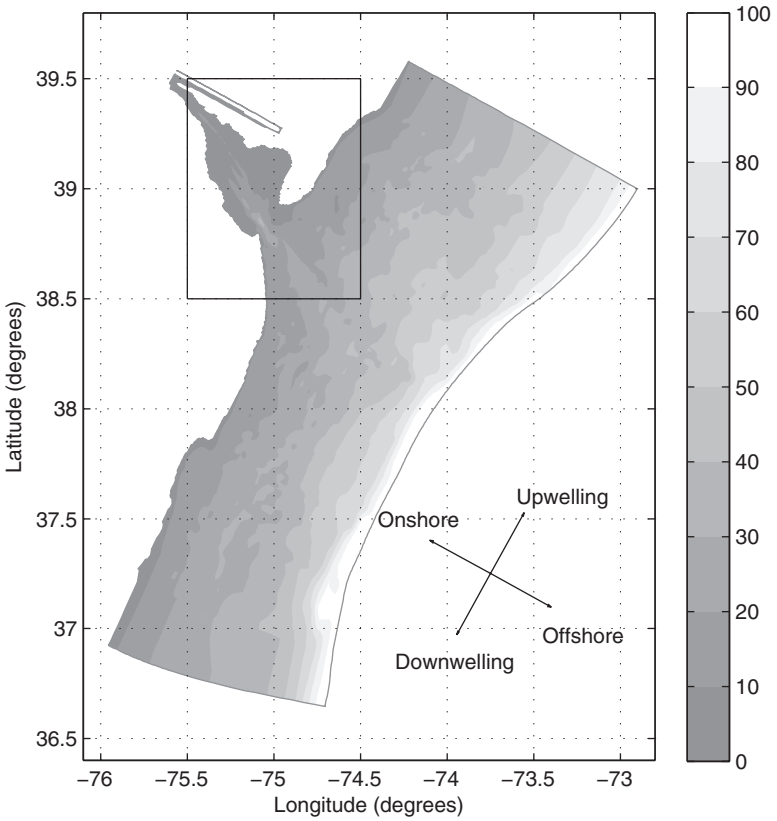

Figure 1. Domain of the circulation model illustrating bottom bathymetry (m). Black rectangle indicates region shown in Figures 3 and 10. Arrows show direction of wind velocities for onshore, upwelling, offshore, and downwelling winds. Note that the trajectory of the Delaware River has been modified to remain within the model domain. This modification has no effect on the model output.

$$\mathbf{u}_t + \mathbf{u} \cdot \nabla\mathbf{u} + w\mathbf{u}_z + f\mathbf{k} \times \mathbf{u} = -\frac{1}{\rho_o}\nabla P + (K_M\mathbf{u}_z)_z + \nabla(A\nabla\mathbf{u}) \tag{2}$$

$$\rho g = -P_z \tag{3}$$

$$S_t + \mathbf{u} \cdot \nabla S + wS_z = (K_H S_z)_z + \nabla(A\nabla S) \tag{4}$$

where ∇ is the horizontal gradient operator, $\mathbf{u}$ is the horizontal velocity vector (u, v), w is the vertical velocity, P is the pressure, f is the Coriolis parameter, S is the salinity, and ρ_o is a reference density. Temperature is kept constant in all simulations. Density, ρ, is computed from the equation of state. The model uses a recursive advective scheme (Smolarkiewicz and Grabowski, 1990) that reduces diffusive artifacts associated with advection and the Mellor-Yamada level 2.5 closure scheme to calculate the vertical eddy viscosity, K_M, and diffusivity,

K_H. The background vertical eddy viscosity in the closure scheme is $2 \times 10^{-5}\,\mathrm{m^2\ s^{-1}}$. Decreasing or increasing the background value by an order of magnitude has no effect on the simulations. The parameter A represents both the horizontal eddy viscosity and diffusivity and is calculated using the Smagorinsky (1963) diffusion formula:

$$A = C_a \Delta x \Delta y \left(\left(\frac{\partial u}{\partial x} \right)^2 + \left(\frac{\partial v}{\partial y} \right)^2 + \frac{1}{2} \left(\frac{\partial u}{\partial x} + \frac{\partial v}{\partial y} \right)^2 \right)^{1/2} \tag{5}$$

where Δx, Δy are the horizontal grid sizes and C_a is a constant equal to 0.1 (Whitney and Garvine, 2006).

The surface boundary condition for velocity is

$$(K_M \mathbf{u})_z = \frac{\boldsymbol{\tau}^s}{\rho_o} \tag{6}$$

where $\boldsymbol{\tau}^s$ is the wind stress vector. The bottom boundary condition for velocity is

$$(K_M \mathbf{u})_z = C_D |\mathbf{u}_b| \mathbf{u}_b \tag{7}$$

where $\mathbf{u}_b$ is the bottom velocity. The drag coefficient, C_D, in Eq. 7 is determined by

$$C_D = \max \left[0.0025, \kappa^2 \left(\ln \left(\frac{\Delta z}{z_o} \right) \right)^{-2} \right] \tag{8}$$

where $\kappa = 0.4$ is the von Karman's constant, Δz is half the vertical grid spacing at the bottom, and $z_o = 0.3$ cm is the roughness height. There is no salt flux at the surface, bottom or land boundaries. A partial slip condition (Whitney and Garvine, 2006) is applied along land boundaries. The offshore boundary is located along the 100 m isobath and its free surface is fixed to the tides by specifying the amplitude and phase of the semi-diurnal M2 tidal constituent derived from an inverse tidal model incorporating TOPEX/Poseidon altimetry data (Egbert *et al.,* 1994). The normal gradients of tangential velocity and salinity are set to zero at this boundary. The across-shelf boundaries at the up- and downshelf locations are combination clamped/radiation boundaries that are specifically developed for tidal, wind, and buoyancy forcing (Chapman, 1985; Whitney and Garvine, 2006).

Since ECOM3d is a sigma-level (or terrain-following) model, the vertical resolution is proportional to water depth. This simulation contains 15 sigma (σ) levels whose spacing is much closer near the surface and the bottom boundaries (5% of the water column) than the middle of the water column (15%) to better resolve the surface and bottom Ekman layers. The model grid contains 300×150 cells covering a $340\ \mathrm{km} \times 240\ \mathrm{km}$ area. The horizontal grid size for the simulation varies from 0.75 km within Delaware Bay to 3 km on the shelf. However near the boundaries grid sizes increases to 8 km. The model uses a split time step of 9.2 s for the barotropic mode and 92 s for the baroclinic mode.

In our study, the model was forced with freshwater discharge obtained from daily records of river flow at a United States Geological Survey gauging station located above the head of the estuary at Trenton, New Jersey (Fig. 2A). The wind velocities (Fig. 2B) that

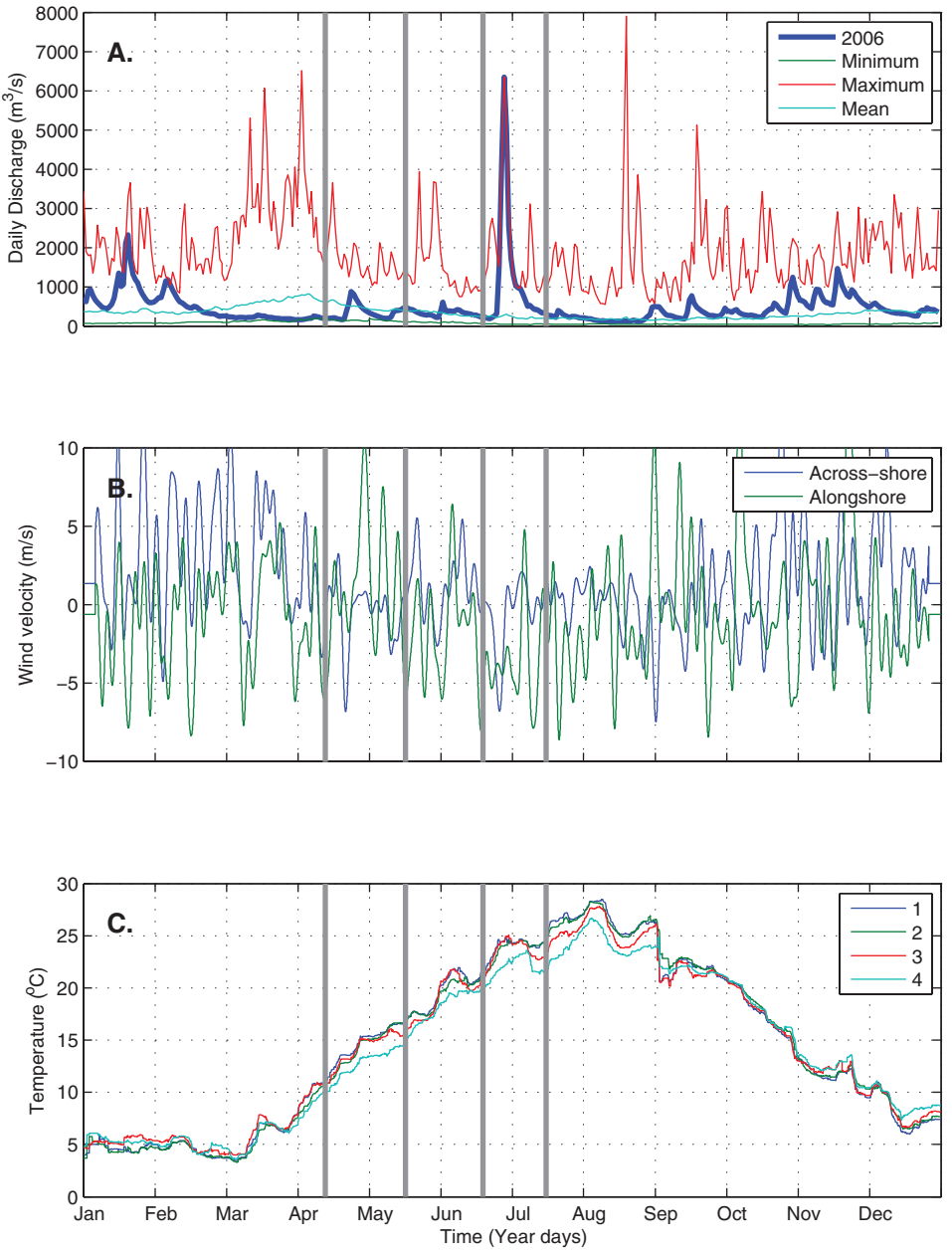

Figure 2. Forcing functions of circulation and larval behavior models for 2006. (A) Discharge of Delaware River measured at Trenton, NJ gauging station for 2006 (blue line). Daily maximum values are shown in red. Minimum values are shown in green. Mean values are shown in light blue. (B) Across-shore (blue) and alongshore (green) wind velocities measured at Environmental buoy 44007. (C) Temperatures at the four spawning sites shown in Figure 3. Vertical gray lines in each panel represent times of spawning for the model.

were used to force the model were obtained from a blend of hourly surface observations at NOAA Environmental Buoy #44009 (located approximately 50 km southeast of Delaware Bay) and the Atlantic City International Airport (located approximately 100 km north of Delaware Bay). During times when both stations were recording, a numerical average of the two observations was used to calculate model wind velocities. When only one station was recording, that one was used to calculate the model wind velocities. Once calculated, the wind velocities were filtered using a Lanczos low-pass filter with a cut-off frequency of 1/40 hour^{-1}.

The circulation model was run from 1988–2006. The simulation began with a period of tidal forcing for 120 tidal cycles before river discharge and winds were imposed. With the introduction of river and wind-forcing, a salinity field was imposed that was based on an along-estuary salinity trend derived by Garvine *et al.* (1992). The initial conditions reach quasi steady-state after a few weeks (Whitney and Garvine, 2006). The extensive spin-up time of the model allowed the inclusion of real-world observations in 1993 and 2003 as well as adjustment of the flow field to the forcing agents on a relatively long time scale (Whitney and Garvine, 2006; Tilburg *et al.,* 2007b). Flow fields for the year 2006 as well as a number of idealized cases were then used as input for the particle advection scheme. The year 2006 was specifically chosen to provide an example of realistic temporal variations in both winds and river of a typical year. River discharge and winds in 2006 were typical of the region but did include a large discharge event at the end of June.

c. Larval advection model

The trajectories of the simulated larvae were created using a particle advection scheme that tracked larvae released into the model flow field using a simple fourth-order Runge Kutta method (e.g. Hannah *et al.,* 1998; Tilburg *et al.,* 2005). Since the swimming speed of *E. sinensis* zoeae is much less than the horizontal velocities of the flow field, the larvae were modeled as passive particles in the horizontal plane. However, swimming behavior in the vertical direction was included in simulations that investigated the role of vertical shear in larval transport. In these simulations, the larvae were modeled as particles that could change depths according to a set of prescribed behaviors. However, advection was solely by horizontal velocities. The position of any larva can be written as:

$$\mathbf{x}_i(t + \Delta t) = \mathbf{x}_i(t) + \mathbf{u}_i(t) \cdot \Delta t + \mathbf{x}'_i(t) \tag{9}$$

in which $\mathbf{x}_i(t)$ represents the horizontal position vector (x, y) of the ith larvae at time t, $\mathbf{u}_i(t)$ represents the local horizontal velocity and $\mathbf{x'}_i(t)$ represents the sub-grid scale processes not resolved by the numerical model. The sub-grid scale processes were approximated using the random walk formulation of Visser (1997) that is expressed as:

$$\mathbf{x}'_i(t) = \nabla A(\mathbf{x}_i(t)) \cdot \Delta t + R(2r^{-1}A(\mathbf{x}_i(t) + 1/2\nabla A(\mathbf{x}_i(t)) \cdot \Delta t) \cdot \Delta t)^{1/2} \tag{10}$$

where $r = 1/3$ and R is a random process with zero mean and unit variance. Comparison of the random walk formulation (Eq. 10) and simple advection of the particles revealed few

differences in the aggregate analysis of the particles, which is consistent with a flow regime in which advection is the dominant transport process. The time step used in the larval advection model (2484 s) was chosen as a balance between computational efficiency and numerical accuracy; halving the time step to 1242 s showed no appreciable difference in the larval trajectories.

If a larva was transported onto land by the advection scheme, it remained at the boundary between land and water until the flow direction resulted in movement back into the flow field. Larvae that encountered the land/water boundary after day 30 were assumed to undergo settlement and metamorphosis (Dittel and Epifanio, 2009). Larvae that left the model domain through an open boundary in the coastal ocean were removed from the simulation.

Since this study examines the effects of several different vertical swimming behaviors on the transport of larvae, larvae could occupy multiple depths. Surface larvae were advected by horizontal velocities at the shallowest sigma level ($\sigma = 0$), and near-bottom larvae were advected by horizontal velocities at the deepest sigma level that was characterized by non-zero velocities ($\sigma = -0.95$ or 5% off the bottom). Vertical velocities for zoeae typically range between 1 and 5 mm s^{-1} (Forward, 1990; Epifanio, 2007; Houser and Epifanio 2009). Since the time step for the larval advection scheme was 2484 s and the depth of Delaware Bay generally varies between 10–20 m, vertical migration would generally occur over two to three time steps (3×2484 s $= 7452$ s). Consequently, we allowed larvae to occupy the middle of the water column ($\sigma = -0.5$) for one time step during the simulated vertical migration to provide for realistic vertical and horizontal movement. Vertical mixing is an important process that is typically incorporated into larval transport studies in estuaries (e.g. Tilburg *et al.,* 2010); however, our study specifically neglects vertical mixing for two reasons: (1) the vertical movement of larvae due to mixing is much smaller than that due to vertical migratory behavior and (2) the object of this study is to examine the full range of larval settlement due to different vertical migration schemes.

A simple scaling argument reveals that the advection of larvae due to vertical swimming is significantly greater than that due to vertical mixing. The vertical movement of a larva over one time step due to vertical mixing can be scaled as $\frac{K_M}{H}\Delta t$ where H is the depth of the estuary. The movement of a larva due to vertical swimming can be scaled as $w_{swim}\Delta t$. The relative contributions of the two mechanisms can be estimated by their ratio: $\frac{K_M}{Hw_{swim}}$ where large values indicate a strong contribution from mixing and small values indicate greater contribution from vertical swimming. Typical values of K_M for estuaries ($1 \times 10^{-4} - 5 \times 10^{-4}$ m^2 s^{-1}, e.g. Hetland and Geyer, 2004), vertical swimming speeds of larvae (1–5 mm s^{-1}, e.g. Houser and Epifanio 2009), and the depth of the estuary (10 m) produce values for the ratio that range from 0.002 to 0.05, indicating that vertical swimming is a much larger contributor to vertical movement of larvae than mixing.

Any amount of physical vertical advection and mixing would tend to *reduce* the effects of different vertical behaviors and decrease the range of potential settlement scenarios.

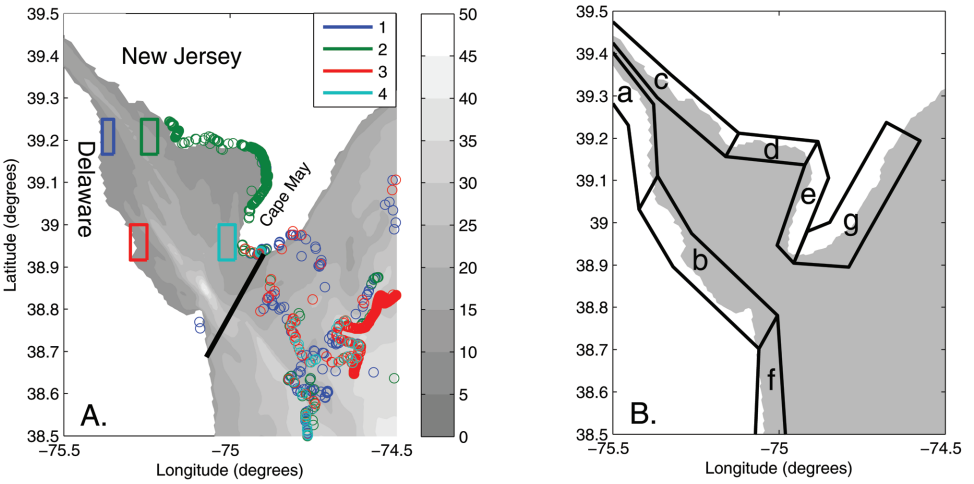

Figure 3. (A) Location on June 12, 2006 of individual particles (open circles) advected by the larval behavior model that were spawned on May 18, 2006 from each spawning site (rectangles) shown on bottom bathymetry (m). The black line at the bay mouth represents the division between Delaware Bay and the coastal ocean. (B) Settlement zones used to determine coastal settlement locations of larvae.

Since we do not know the actual migratory behavior of mitten crab larvae, we purposefully neglected even the small amount of vertical mixing to *enhance* the difference between the vertical migration schemes and determine the *full* range of larval settlement possibilities due to different migratory behavior.

Larval hatching was simulated in the model as the instantaneous placement of particles at the surface in four separate locations (Fig. 3A) within Delaware Bay where adult mitten crabs are likely to release larvae (Dittel and Epifanio, 2009). These sites were chosen to span a range of geographic locations and hydrodynamic conditions, ranging from weak tidal, strong buoyancy-driven flow at site 1 to strong tidal flow near the mouth at site 3 to the relatively quiescent conditions upstream (site 2) and near the northern terminus of the bay (site 4). Larval release in *E. sinensis* typically occurs when temperatures exceed 10°C (see review by Dittel and Epifanio, 2009), and for our study, we chose four separate times for spawning during 2006 in which the observed temperatures exceeded 10°C (Fig. 2C). Each spawning time was characterized by a different pattern of river discharge and wind forcing (Fig. 2A, B). The simulations were run for 85 days to encompass the maximum possible larval duration (see review by Dittel and Epifanio, 2009). In a separate set of analyses, we determined the proportion of larvae that remained within the bay after each time step in the simulations, as well as the proportion of larvae that encountered any one of seven coastal "settlement zones" by the end of each simulation (Fig. 3B).

Previous numerical modeling studies (e.g. Garvine *et al.,* 1997; Tilburg *et al.,* 2005) have shown that the inclusion of larval mortality can affect the magnitude of settlement

Table 1. Description of simulations.

Simulation name	Wind speed (m/s)	Wind direction*	River discharge (m^3/s)	Larval behavior
R1	Variable (Fig. 2B)	Variable (Fig. 2B)	Variable (Fig. 2A)	Surface dwelling
B	0	N/A	350	Surface dwelling
B_{min}	0	N/A	200	Surface dwelling
B_{max}	0	N/A	Variable to 5780 at peak	Surface dwelling
B_{off}	5	Offshore	350	Surface dwelling
B_{up}	5	Upwelling	350	Surface dwelling
B_{on}	5	Onshore	350	Surface dwelling
B_{down}	5	Downwelling	350	Surface dwelling
B_{diel}	0	N/A	350	Diel migration
B_{tidal}	0	N/A	350	Tidal migration
B_{onto}	0	N/A	350	Ontogenetic migration

*See Fig. 1 for illustration of wind directions.

events but has little effect on timing or location of settlement events. We have neglected mortality in this analysis since (1) we are interested in the effects of different physical forcings and larval behavior on settlement locations, (2) we have no knowledge of larval mortality rates to apply to the larvae, and (3) we have little understanding of the present population size. The inclusion of a parameter in which we have no prior knowledge and which has been shown to have negligible effects on locations of larval settlement (the primary objective of this study) would complicate our analysis.

d. Simulations

We performed a number of realistic and idealized simulations to investigate the effects of various physical and biological factors on larval retention. These included a simulation using observed winds and river discharge for 2006 (referred to as R1 in the text), as well as several idealized simulations that systematically varied river discharge, wind direction, and behavior of the larvae (Table 1). The isolation of individual physical mechanisms has proven effective in both the analysis of physical characteristics of river-plume transport (Xia *et al.,* 2007) and the examination of larval patch dynamics (Tilburg *et al.,* 2007a).

To investigate the effects of variations in river discharge on larval transport and retention, we ran simulations forced by river discharge and tides only. In these simulations, wind stress was set to zero. Three different discharges (B, B_{min}, and B_{max}) were chosen to span a range of different conditions. These included a constant mean discharge (350 m^3/s),

a constant minimum discharge (200 m^3/s), and a maximum discharge event. The maximum event was simulated by mean discharge (350 m^3/s), followed by a rapid increase to 5780 m^3/s after ten days, and an exponential decay back to the mean value over 20 days. The mean and minimum discharge values were calculated from the time series of discharge at the Trenton, NJ gauging station from 1913–2008 (Fig. 2A).

To investigate effects of wind-driven flow on larval transport and retention, we ran the base simulation forced by tides and mean river discharge with constant 5 m/s winds in four directions: onshore (B_{on}), offshore (B_{off}), upwelling (B_{up}), and downwelling (B_{down}). In the coastal ocean, adjacent to Delaware Bay, onshore winds blow from southeast to northwest, offshore winds blow from northwest to southeast, upwelling winds blow from southwest to northeast, and downwelling winds from northeast to southwest (Fig. 1).

Because vertical swimming allows larvae to take advantage of shear in horizontal currents (e.g. Forward *et al.,* 2003), we also investigated effects of larval behavior on transport and retention. We ran a number of simulations that included variations in larval behavior; these idealized simulations were forced by tides and mean river discharge. Since no previous studies had characterized relevant larval behavior of *E. sinensis,* we incorporated into the model several common behaviors that could potentially affect horizontal transport (e.g. Sulkin, 1984; Forward *et al.,* 2003, 2007). All behaviors involved vertical migration only. These models (B_{tidal}, B_{diel}, and B_{onto}) included tidal migration (surface distribution during flood tide and near-bottom distribution during ebb tide), diel migration (surface distribution at night and near-bottom distribution during the day), and ontogenetic migration (surface distribution during the first two weeks after spawning and near-bottom distribution for the duration of larval development).

3. Results

a. Realistic simulations

Figure 3A shows the advection of larvae from each spawning site during the simulation that reproduced the actual physical conditions of 2006 (R1). In this example, larvae were released at each site on May 18, 2006, and the figure shows their location 25 days later on June 12, 2006. Examination of Figure 3A demonstrates that patterns of larval transport are strongly dependent on location of the spawning site. A majority of those larvae released at sites 1, 3, and 4 had already exited the bay by 20 days after spawning (Fig. 4B), but most of those larvae spawned at site 2 (green rectangle in Fig. 3A) were retained near the New Jersey coast of Delaware Bay for the duration of the simulation. The final locations of larvae spawned at other times in 2006 (right panel of Fig. 4) also varied strongly by spawning site.

Examination of the overall pattern of larval retention in the bay (left panel of Fig. 4) and locations of coastal settlement (right panel of Fig. 4) for multiple spawning events shows that the ultimate fate of larvae in the bay is strongly dependent on both time and location of spawning. Larvae spawned on April 14, 2006 were initially affected by a flow field driven

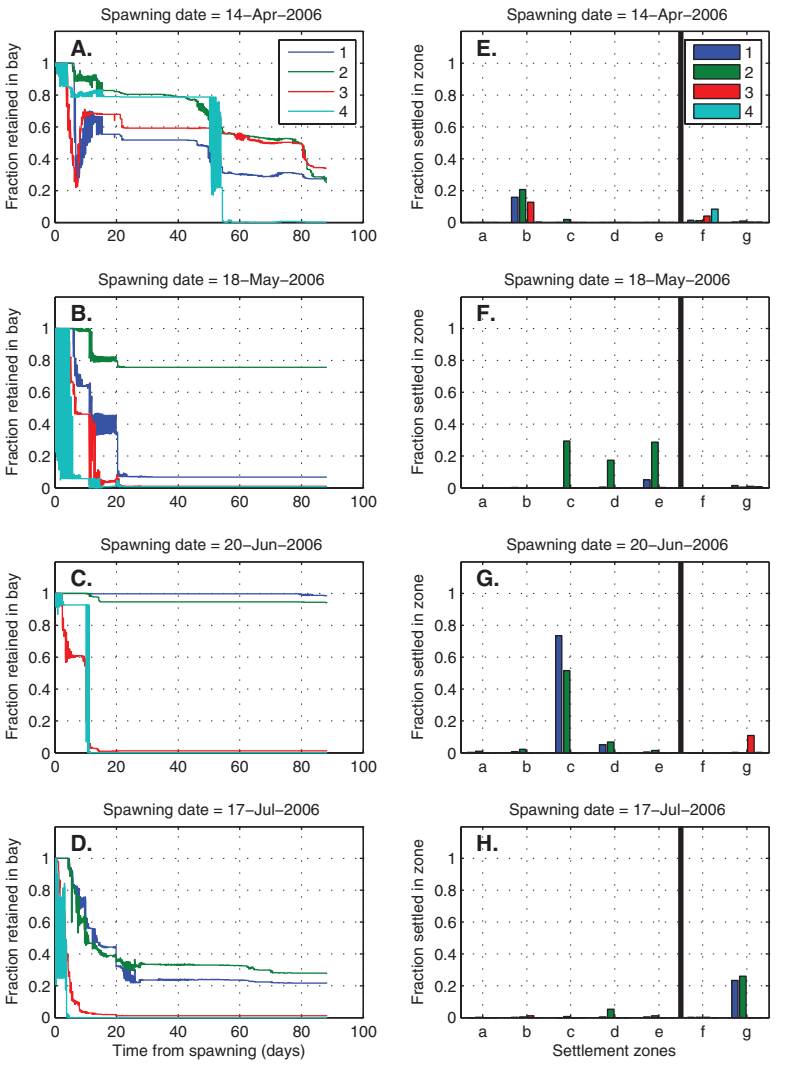

Figure 4. (Left panel) Fraction of particles that remain in Delaware Bay originating at the four spawning sites during the realistic simulation for (A) April 14, 2006, (B) May 18, 2006, (C) June 20, 2006, and (D) July 17, 2006. (Right panel) Fraction of particles that settle in the settlement zones illustrated in Figure 3B 85 days after spawning during the realistic simulation for (E) April 14, 2006, (F) May 18, 2006, (G) June 20, 2006, and (H) July 17, 2006. Zones to the left of the vertical black line correspond to areas inside the bay. Zones to the right correspond to zones outside the bay. Note that the sum of fractions that settle in the settlement zones can be less than one if not all particles settle.

by moderate river discharge and downwelling/onshore winds (Fig. 2). Most of the larvae that were spawned directly in the buoyant discharge (sites 1 and 3) were immediately removed from the bay, although a number of larvae were returned 10 days after spawning

(Fig. 4A). In contrast, retention among larvae spawned in regions less affected by buoyant discharge (sites 2 and 4) was nearly 80% after 40 days of simulated transport. However, after day 50, the subtidal flow forced by river discharge resulted in the removal of more and more larvae. By day 55, all larvae spawned at site 4 were lost to the bay. Limited larval settlement (from sites 1, 2, and 3) occurred primarily on the Delaware shores (zone b) of the bay and coastal ocean (zone f) (Fig. 4E).

The flow field in late May was governed by upwelling (northeastward) winds and weaker discharge. Of the larvae spawned on May 18, 2006, only those released at site 2 had significant retention (Fig. 4B), mostly settling on the New Jersey shore (zones c, d, & e) of Delaware Bay (Fig. 4F). Larvae spawned at the three other sites left the bay by 20 days after spawning. The larvae released on June 20, 2006 were affected by strong upwelling winds and an extremely high river discharge event 10 days after spawning. There was little retention of larvae spawned at the two sites nearest the mouth (3 and 4) after 10 days; however, larvae spawned at the two up-estuary sites (1 and 2) were mostly retained within the bay (Fig. 4C) and settled on the New Jersey shore (zones c and d) (Fig. 4G). Those larvae spawned on July 17, 2006 were subjected to upwelling winds and weak discharge, resulting in the loss of most larvae from the bay (Fig. 4D); however, there was some limited settlement of larvae on the New Jersey shore (zone d) (Fig. 4H). The left panel of Figure 4 shows high-frequency oscillations in the proportion of retained larvae in some segments of the time series. These oscillations occurred during periods of time when simulated larvae were located near the estuary/ocean boundary and were transported back and forth across the boundary with each change of the tide.

b. Discharge

The realistic simulation was based on actual data from 2006 and was driven by a combination of observed tides, river discharge, and wind-driven flow. To examine which of these physical mechanisms were responsible for the variations in retention and settlement, we ran a number of idealized simulations in which river discharge and winds were systematically varied. Initial conditions for each idealized simulation were similar to actual conditions in 2006 for any specified discharge, and the range of discharge and wind spanned the observed values for 2006. Once the simulation had reached statistical steady-state (i.e. average kinetic energy of the flow field is constant), winds (if specified) were introduced for 4 days and the larvae were then released into the flow field. Examination of those simulations in which wind stress was set to zero and river discharge was assigned three different values (B_{mean}, B_{min}, B_{max}) reveals significant variations in retention and settlement of larvae as a function of spawning location (left panel of Fig. 5). Interestingly, larval settlement and retention increased with increased river discharge. Those larvae spawned during mean discharge conditions showed tidal fluctuations in larval retention throughout the simulation, indicating that a number of larvae remained near the mouth of Delaware Bay, leaving the bay during ebb tides but re-entering the bay during flood tides (Fig. 5A). This finding is consistent with results of Tilburg *et al.* (2007a), who

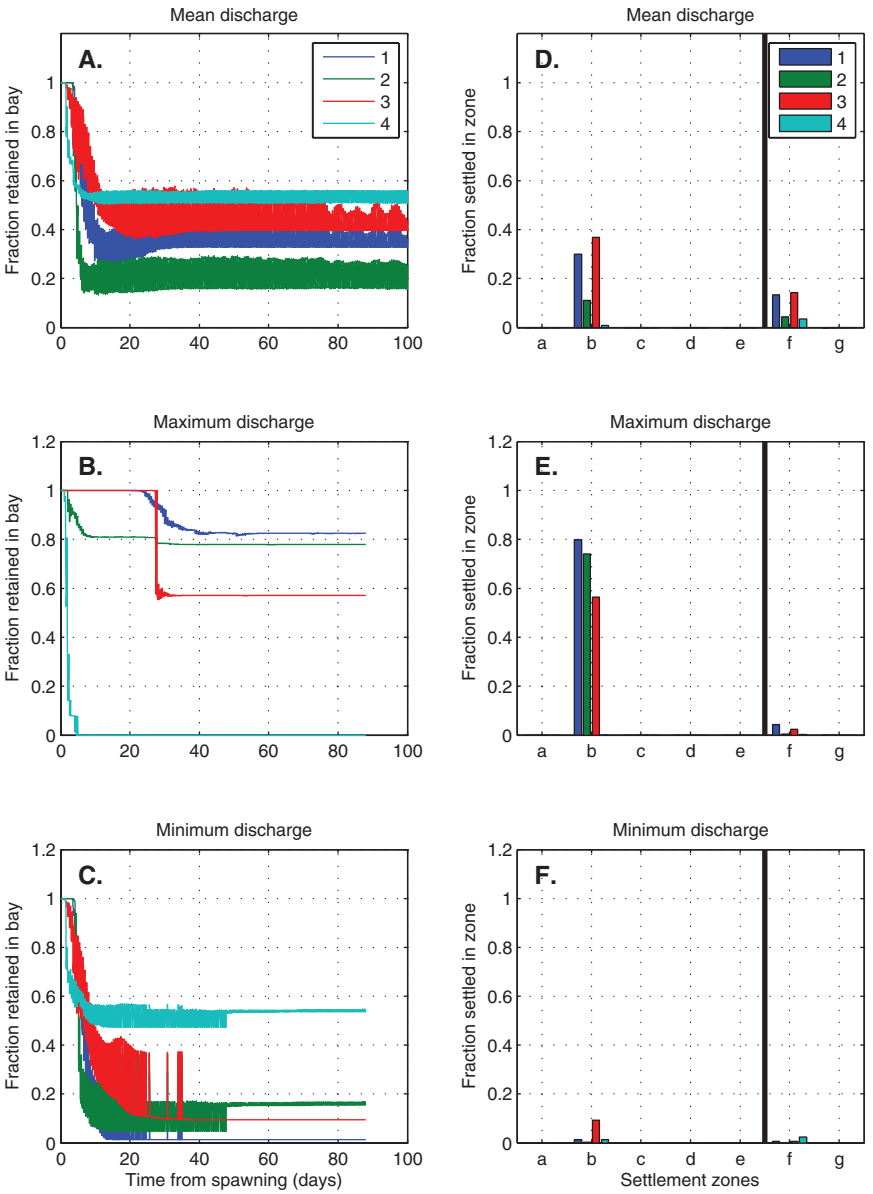

Figure 5. (Left panel) Fraction of particles that remain in Delaware Bay originating at the four spawning sites during simulations with (A) mean discharge (350 m^3/s), (B) maximum discharge (peak of 5780 m^3/s), and (C) minimum discharge (200 m^3/s). (Right panel) Fraction of particles that settle in the settlement zones illustrated in Figure 3B 85 days after spawning for (D) mean discharge, (E) maximum discharge, and (F) minimum discharge.

determined that larvae were aggregated in a surface convergence zone at the mouth of Delaware Bay, which was formed by the seaward movement of the river discharge into the ambient coastal ocean.

There was limited settlement on the Delaware shores (zones b and f) of the bay and coastal ocean (Fig. 5D). The flow field generated by maximum discharge (Fig. 5B) resulted in greater retention of larvae than the mean discharge simulation for three of the spawning sites (1, 2 and 3). Larvae from these sites all settled in greater numbers on the Delaware shore (zone b) of the bay (Fig. 5E). However, maximum discharge conditions did result in the almost immediate removal of the larvae spawned nearest the bay mouth (site 4). This result is consistent with the realistic simulation on June 20, 2006, in which those larvae spawned before an extremely large discharge event exceeded the retention of larvae forced by more moderate discharges (Fig. 4). In contrast, those larvae released in the flow field forced by minimum river discharge resulted in the least amount of retention (Fig. 5C) and settlement (Fig. 5F). Interestingly, site 4 in all three simulations resulted in little settlement, despite exhibiting the highest retention of all sites during mean and minimum discharge simulations.

c. Winds

Examination of those simulations forced by mean discharge with varying wind directions (Fig. 6) reveals that winds are the primary agent controlling proportional retention of surface-dwelling larvae in the bay. In the absence of strong river discharge, winds often resulted in transport of the larvae to the shores of the bay. Onshore winds yielded total retention for all spawned larvae (Fig. 6A), regardless of spawning location. All larvae spawned at sites 1, 2, and 3 were transported up-estuary in subtidal flow forced by the wind. These larvae encountered the Delaware shore of the bay (zones a and b) where they remained (Fig. 6E). Those larvae spawned at site 4 were retained in the bay but did not settle in a coastal location. Instead, they remained within the water column in the bay.

Offshore winds resulted in all larvae from sites 1, 2, and 3 moving down-estuary and leaving the bay (Fig. 6B). Again, those larvae spawned at site 4 remained within the water column, but inside the bay (Fig. 6F). Downwelling winds provided total retention for all but spawning site 4 (Fig. 6C). Larvae released at locations 1, 2, and 3 were simply advected downwind to the Delaware shore (zones a and b) of the bay (Fig. 6G). The larvae spawned at site 4 entered the buoyant discharge. Some settled on the Delaware shore (zone b), but most were advected out of the bay before continuing downshelf (southward), where some settled on the Delaware shore of the coastal ocean (zone f). Upwelling winds did not result in a major loss of larvae from the bay (Fig. 6D) as might be expected from Ekman transport (e.g. Epifanio and Garvine, 2001) but instead transported the larvae spawned at sites 1 and 2 to the New Jersey shore (zones c and d) of the bay (Fig. 6H). A small number of those larvae spawned at site 3 (located directly within the buoyant discharge) remained within the buoyant current and were transported out of the bay before moving upshelf of the region. Interestingly, the remainder of the larvae spawned at site 3 (along with all of the

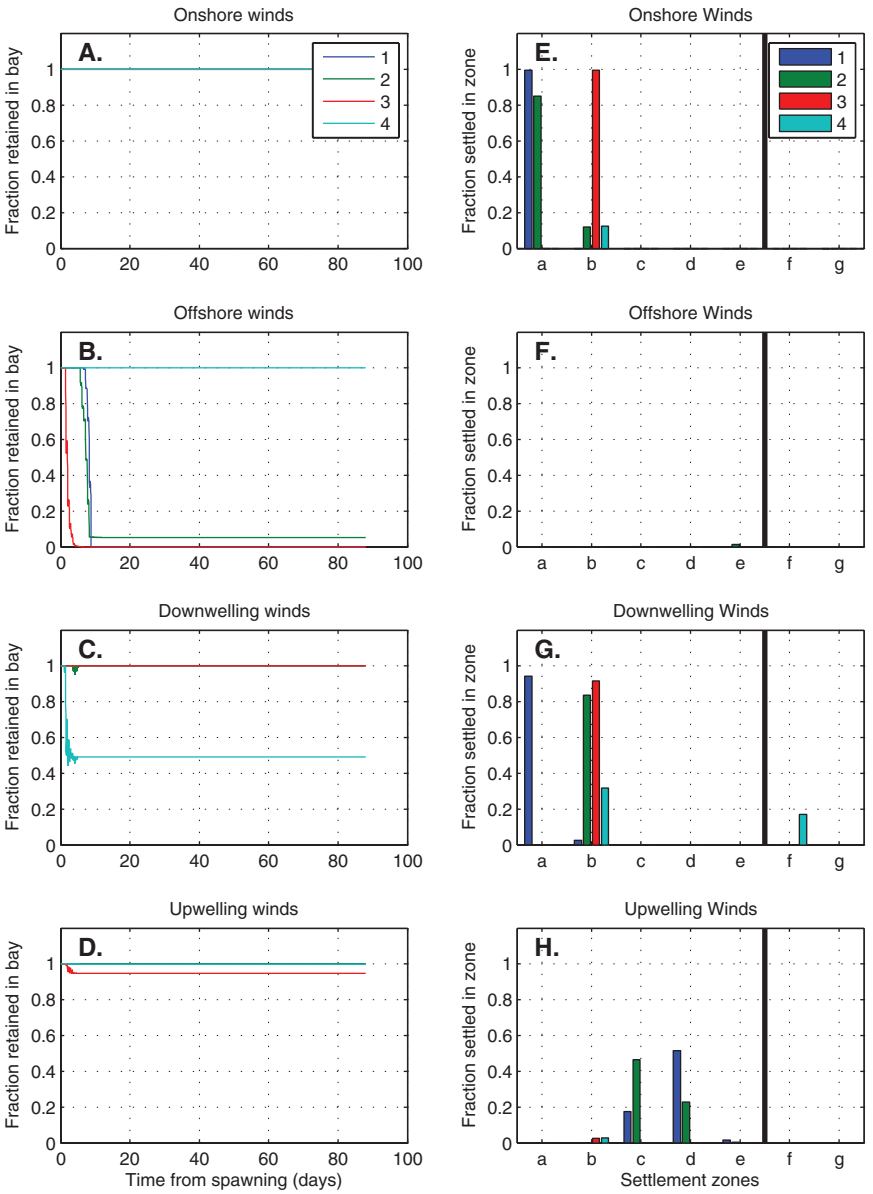

Figure 6. (Left panel) Fraction of particles that remain in Delaware Bay originating at the four spawning sites during mean discharge and constant (A) onshore winds, (B) offshore winds, (C) downwelling winds, and (D) upwelling winds of 5 m/s. (Right panel) Fraction of particles that settle in the settlement zones illustrated in Figure 3B 85 days after spawning during (E) onshore winds, (F) offshore winds, (G) downwelling winds, and (H) upwelling winds. Note that the overlap of lines in A, C, and D from sites with complete retention result in not all lines appearing in the figure.

larvae spawned at site 4) remained within the water column and did not settle in any coastal location.

d. Larval behavior

The results described above were obtained by tracking larvae that remained in the surface layer. Examination of simulations that incorporated idealized behavior revealed that vertical migration can greatly modify the effects of physical transport mechanisms (Fig. 7). Migration at tidal frequency resulted in complete retention of larvae in the bay, regardless of spawning location (Fig. 7A). However, spawning location was paramount in determining where larvae reached the coast. Some of the larvae spawned at site 1 settled on the up-estuary Delaware shores of the bay (zone a), although the majority remained within the water column. All larvae spawned at sites 3 and 4 and the majority of the larvae spawned at site 2 settled on the down-estuary Delaware shores (zone b) of the bay (Fig. 7D). Diel vertical migration had a smaller effect on transport (Fig. 7B), and retention was only slightly greater than for surface dwelling larvae (Fig. 5A). Settlement was also similar (Fig. 7E), occurring on the Delaware shores of the lower bay (zone b). Retention of larvae undergoing ontogenetic vertical migration was slightly more than for surface larvae at mean discharge at sites 1, 2, and 3 (Fig. 7C), but patterns of settlement were similar (Fig. 7F).

Since the vertical migratory behavior of *E. sinensis* is not known, the effects of different behavior and variations in the physical forcings were directly compared (Figs. 8 and 9). Examination of the effects of variations in both larval behavior and river discharge (Fig. 8) revealed that different larval behavior did not affect spatial patterns of larval settlement under identical discharge conditions, but varying discharge conditions had large effects on larval settlement for identical behavior. Diel migration (third column of Fig. 8) and ontogenetic migration (fourth column) resulted in very similar settlement patterns to surface larvae (first column) for all discharges. Tidal migration (second column) resulted in the greatest differences in settlement. Tidal migrating larvae settled in greater numbers, but at similar locations, than other migratory behaviors. The one large difference was that migrating larvae spawned at site 4 were more likely to settle than other behaviors.

Examination of the effects of larval behavior and wind forcing (Fig. 9) also revealed much greater effects of wind-forced transport than larval behavior on larval settlement locations. Diel (third column of Fig. 9) and ontogenetic (fourth column) migration resulted in similar settlement magnitude and location to surface dwelling larvae. Again, tidal migration of the larvae (second column of Fig. 9) resulted in greater settlement. Offshore winds (second row of Fig. 9) resulted in significant settlement of only tidally migrating larvae. During onshore winds (first row of Fig. 9), tidal and diel migration resulted in more settlement of larvae spawned at site 4 than other behavior.

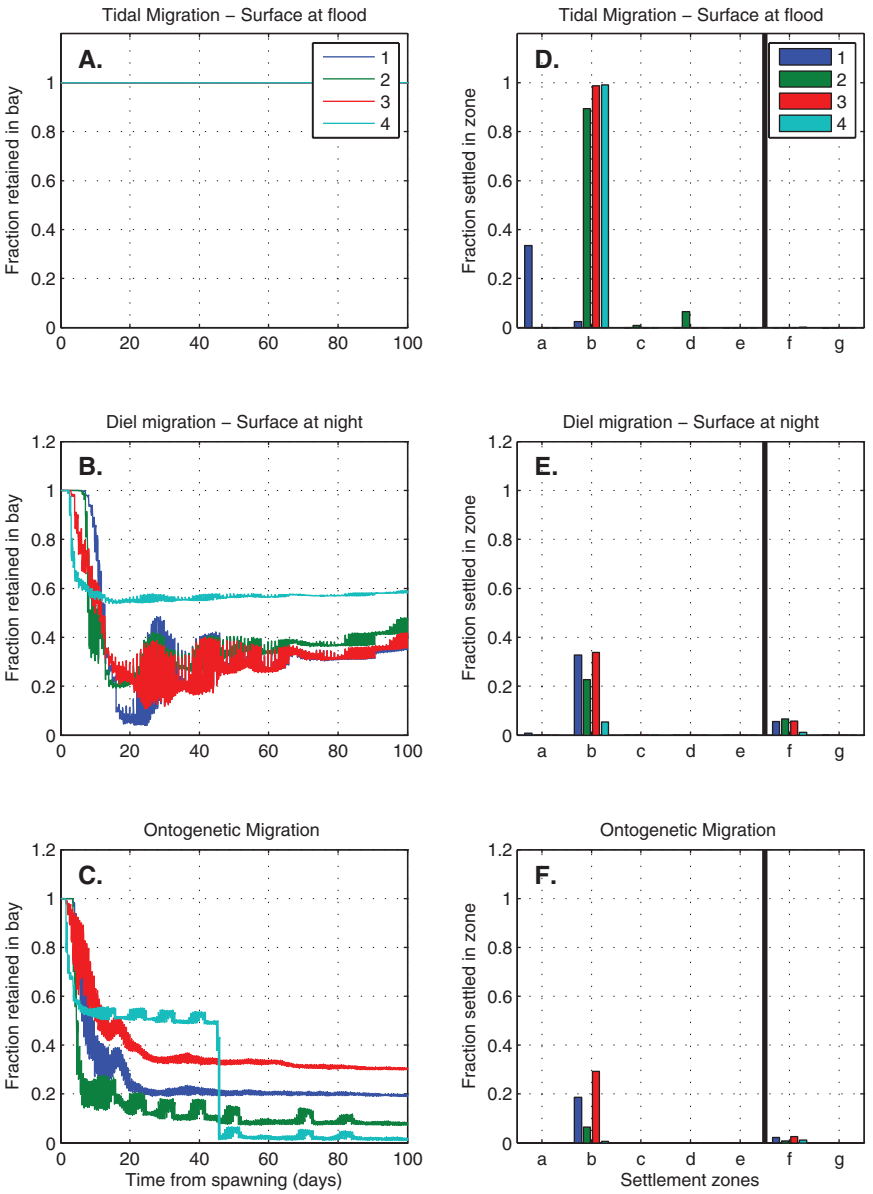

Figure 7. (Left panel) Fraction of particles that remain in Delaware Bay originating at the four spawning sites during mean discharge and specified larval behavior, including (A) tidal migration resulting in particles at the surface during flood tide, (B) diel migration resulting in particles at the surface at night, and (C) ontogenetic migration resulting particles at surface during the first two weeks after spawning and particles residing at the bottom for the duration of their development. (Right panel) Fraction of particles that settle in the settlement zones illustrated in Figure 3B 85 days after spawning for (D) tidal migration, (E) diel migration, and (F) ontogenetic migration. Note that the overlap of lines in A from sites with complete retention result in not all lines appearing in the figure.

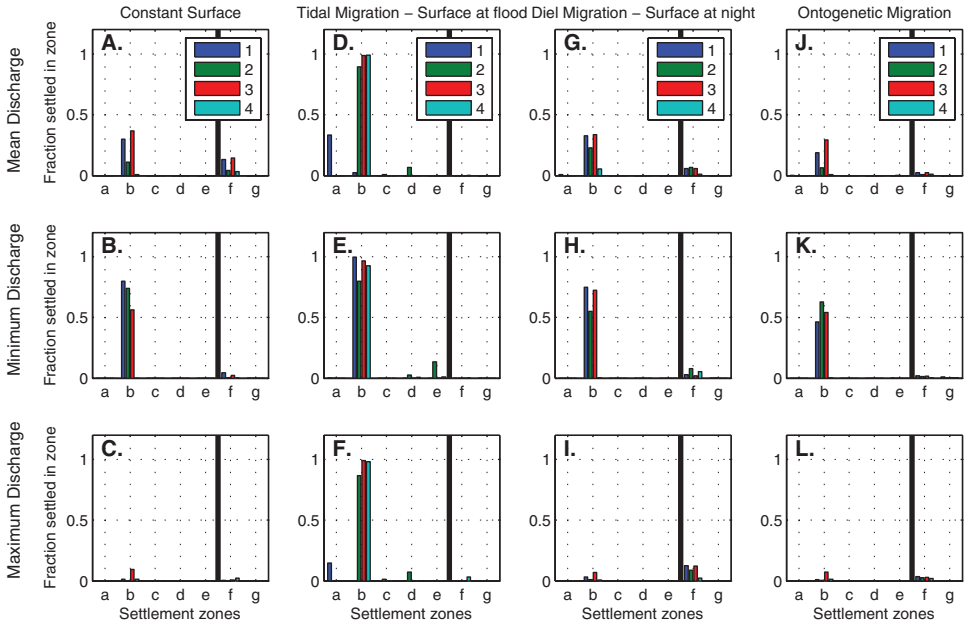

Figure 8. Fraction of particles that settle in the settlement zones illustrated in Figure 3B 85 days after spawning for different discharges (rows) and larval behavior (columns).

4. Discussion

Results from these simulations reveal that changes in the time and location of spawning can result in large variations in retention and settlement of mitten crab larvae in Delaware Bay. The realistic simulations in our study showed that larvae spawned in the buoyancy-driven current or near the mouth of the bay (subject to strong tidal currents) have a greater likelihood of leaving the bay. Those larvae that are spawned in the northern portion of the bay, which are not exposed to strong currents, are more likely to be retained in the bay. This is in agreement with the numerical study by Tilburg *et al.* (2007a) who found that blue crab larvae spawned in buoyancy-driven flow at the mouth of Delaware Bay were not likely to return as megalopae. Detailed analysis of the various scenarios in the present investigation showed that variations in river discharge and wind direction can greatly affect these general results, resulting in settlement on either side of the bay.

Onshore and downwelling winds resulted in almost total retention of larvae within the bay, and most larvae spawned at sites 1, 2, and 3 settled on the Delaware shore of the bay. Upwelling winds resulted in high larval retention also, but settlement on the New Jersey shore of the bay. Offshore winds resulted in most larvae leaving the bay. Again the strong relationship between winds and larval settlement agrees with previous studies of blue crabs and other planktonic larvae. Both the numerical study of Garvine *et al.* (1997) and the observational study of Jones and Epifanio (1995) found that the settlement of blue crab

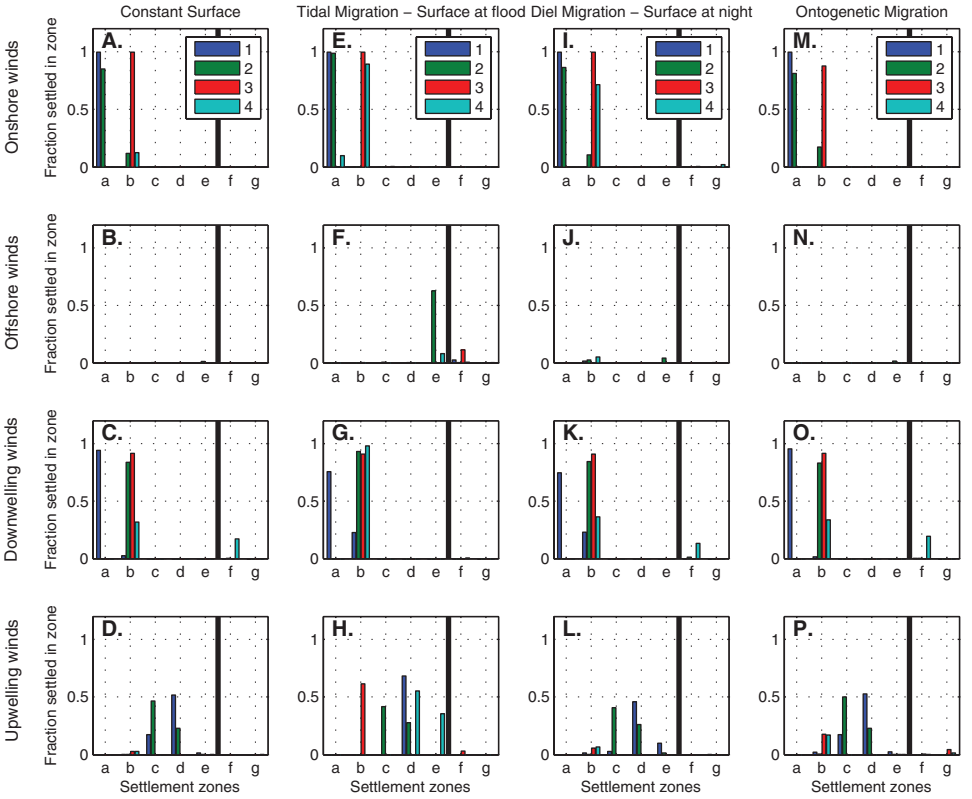

Figure 9. Fraction of particles that settle in the settlement zones illustrated in Figure 3B 85 days after spawning for different wind conditions (rows) and larval behavior (columns).

megalopae in Delaware Bay occurred during downwelling events. Modeling studies by Blanton *et al.* (1999) and Tilburg *et al.* (2005) also found that onshore winds resulted in larval movement into bays and inlets. Overall, the results of these various modeling studies are consistent with observations of transport in Delaware and Chesapeake bays, which showed that onshore wind events yielded up-estuary surface transport (Janzen and Wong, 2002) and increased ingress of blue crab megalopae (Olmi, 1995).

An unexpected and counter-intuitive result of our modeling study is that greater discharge produced greater overall larval retention and settlement. Examination of larval trajectories for high (B_{max}) and low (B_{min}) discharge simulations over the first twelve days after spawning (Fig. 10) reveals that the majority of larvae that remain within the bay do so because of advection onto the bay shores. This larval advection is directly related to horizontal mixing: the horizontal instabilities associated with the greater velocities produced by larger discharges result in greater horizontal shear and, therefore, greater mixing (Tilburg *et al.,* 2006). This mixing produces more lateral movement of the larvae within the estuary, resulting in a greater likelihood of their encountering the shoreline and

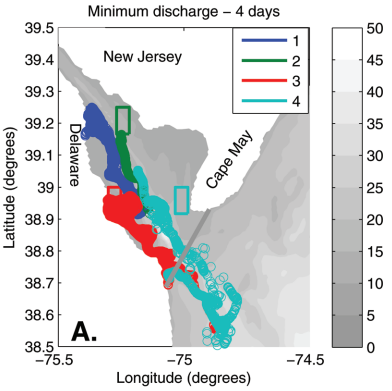
Minimum discharge – 4 days
New Jersey
Delaware
Cape May
1
2
3
4
A.
Latitude (degrees)
Longitude (degrees)
39.5
39.4
39.3
39.2
39.1
39
38.9
38.8
38.7
38.6
38.5
−75.5
−75
−74.5
50
45
40
35
30
25
20
15
10
5
0

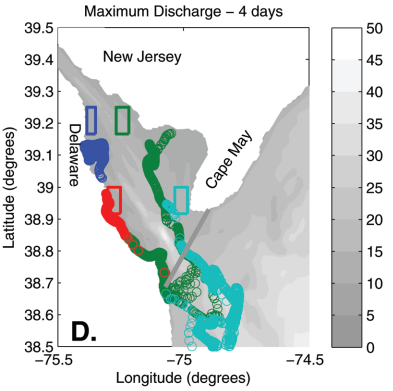
Maximum Discharge – 4 days
New Jersey
Delaware
Cape May
D.
Latitude (degrees)
Longitude (degrees)
39.5
39.4
39.3
39.2
39.1
39
38.9
38.8
38.7
38.6
38.5
−75.5
−75
−74.5
50
45
40
35
30
25
20
15
10
5
0

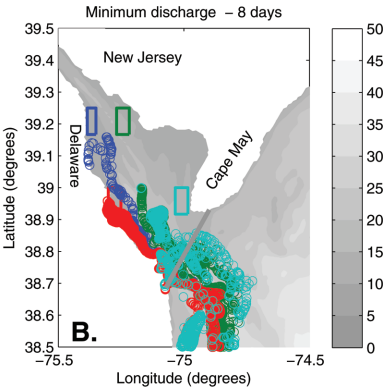
Minimum discharge – 8 days
New Jersey
Delaware
Cape May
B.
Latitude (degrees)
Longitude (degrees)
39.5
39.4
39.3
39.2
39.1
39
38.9
38.8
38.7
38.6
38.5
−75.5
−75
−74.5
50
45
40
35
30
25
20
15
10
5
0

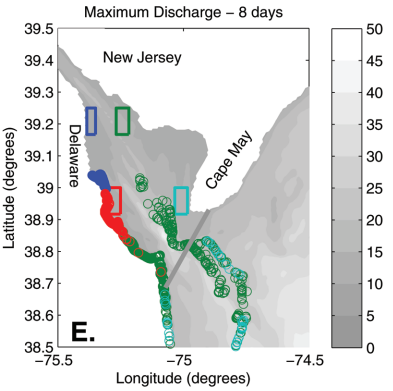
Maximum Discharge – 8 days
New Jersey
Delaware
Cape May
E.
Latitude (degrees)
Longitude (degrees)
39.5
39.4
39.3
39.2
39.1
39
38.9
38.8
38.7
38.6
38.5
−75.5
−75
−74.5
50
45
40
35
30
25
20
15
10
5
0

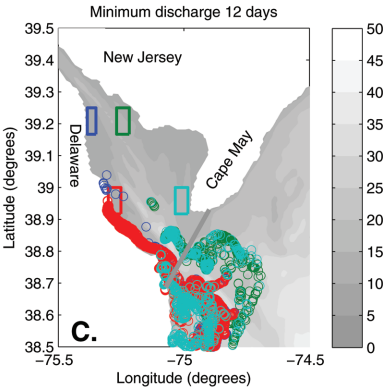
Minimum discharge 12 days
New Jersey
Delaware
Cape May
C.
Latitude (degrees)
Longitude (degrees)
39.5
39.4
39.3
39.2
39.1
39
38.9
38.8
38.7
38.6
38.5
−75.5
−75
−74.5
50
45
40
35
30
25
20
15
10
5
0

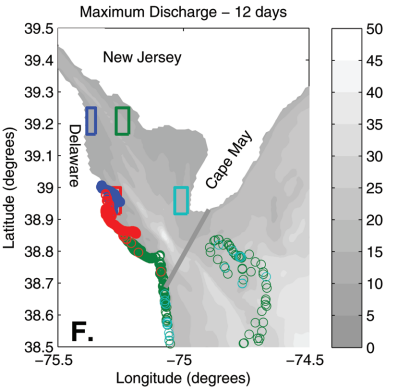
Maximum Discharge – 12 days
New Jersey
Delaware
Cape May
F.
Latitude (degrees)
Longitude (degrees)
39.5
39.4
39.3
39.2
39.1
39
38.9
38.8
38.7
38.6
38.5
−75.5
−75
−74.5
50
45
40
35
30
25
20
15
10
5
0

then settling in the bay. Larvae spawned within the buoyant flow (sites 1 and 3) almost immediately encounter the shoreline of Delaware when subjected to maximum discharge velocities (Fig. 10D) but move much farther downstream when subjected to minimum discharge (Fig. 10A–C), allowing for their removal from the bay. This strong relationship between larval retention and increased river discharge is especially important since climate change scenarios consistently predict increased precipitation and, therefore, increased river discharge in the northeast US (Najjar *et al.,* 2010). This finding suggests that climate change could result in more opportunities for mitten crabs to be retained in bays and estuaries.

Since little is known about the swimming behavior of mitten crabs (Dittel and Epifanio, 2009), earlier studies that examined the fate of larvae in Delaware Bay may not be applicable to mitten crabs. To examine a realistic range of scenarios, the behavioral simulations were purposefully general. We determined the effects of three common vertical migration behaviors that result in larval retention (Sulkin, 1984). The effects of the respective behavioral scenarios on retention and settlement magnitudes (although not settlement locations) were substantial, even though the ambient physical conditions were identical in each simulation. Tidal migration resulted in complete retention of larvae in the bay, regardless of spawning site. This retention is expected since the larvae reside at the surface (where currents were strongest) during the onshore flow associated with the flood tide and at depth (where currents were weakest) during the offshore flow associated with ebb tide (Forward and Tankersley, 2001; Forward *et al.,* 2003, 2007).

Diel migration resulted in similar or slightly greater retention than a constant surface position for all spawning sites. Since diel vertical migration is not in phase with tidal fluctuations, large differences from surface distribution would not be expected. However, daily movement of larvae to the bottom where subtidal buoyancy driven currents were weakest did result in slightly greater retention. Interestingly, large fortnightly fluctuations, corresponding to interaction between the 12.42 hr M2 tides and the 12 hr daily vertical migration, are evident in the time series of larval retention (Fig. 7B).

Ontogenetic migration also resulted in similar or greater retention than surface behavior for larvae spawned at sites 1, 2, and 3. The tidal frequency fluctuations in retention for the ontogenetic migration were much smaller after two weeks (Fig. 7C) when the larvae moved to the bottom where tidal velocities were weaker. Although the larvae were confined to the bottom, the subtidal seaward flow associated with the river discharge still resulted in the removal of the larvae from the bay. This result is consistent with a number of studies that have shown that discharge from Delaware Bay is not confined to the surface

←

Figure 10. (Left panel) Location of individual particles (open circles) shown on bottom bathymetry during the minimum discharge simulation (A) four days, (B) eight days, and (C) twelve days after spawning. (Right panel) Location of individual particles (open circles) during the maximum discharge simulation (D) four days, (E) eight days, and (F) twelve days after spawning.

layers but continues to the bottom (Yankovsky and Chapman, 1997; Wong and Münchow, 1995). The effect of this deep-water discharge is seen in the abrupt decline in retention of site 4 larvae after day 45 (Fig. 7C). The surface flow transported a number of the larvae to the convergent zone at the mouth of the bay (Tilburg *et al.,* 2007a), resulting in tidal frequency variations in retention (Fig. 5A). However, convergence of the buoyant flow is much greater at the surface than at depth in coastal currents (Chapman and Lentz, 1994) and those larvae that migrated to the bottom due to ontogenetic migration did not remain at the center of the bay mouth and were lost to the bay around day 45 (Fig. 7C).

Although the larval behavior affected the *magnitude* of larval settlement, it did not significantly affect the *locations* of settlement. Examinations of variations in larval behavior and the different physical mechanisms showed that variations in the flow field had a much greater effect on the location of settlement. This lack of a strong link between vertical migratory behavior and larval settlement locations should be expected in a weakly stratified estuary (Garvine, 1991), in which currents typically decrease (but may not reverse) with depth. This allows us to examine the effects of the physical flow field during the mitten crab's spawning season on larval settlement, despite little knowledge of the vertical migratory behavior of the larvae.

The effects of the physical characteristics of the flow field on larval transport provide an explanation for the strong seasonal variations in larval retention in the realistic simulations of 2006. The general retention of larvae spawned in early spring (April 14) is due to the mean discharge conditions and to downwelling/onshore winds. The wind-driven transport tended to retain the larvae within the bay; however, the moderate buoyancy-driven subtidal flow eventually removed the larvae from the bay. The loss of larvae from three spawning sites in the late spring simulation (May 18) was due to the upwelling/offshore winds. Those larvae that were retained within the bay were spawned up-estuary (site 2) and were advected onto New Jersey shore. Larvae released in early summer (June 20) were affected by strong upwelling winds and an extremely high river discharge event ten days after spawning. As might be expected, there was little retention of larvae spawned at the two sites nearest the mouth (3 and 4) two or three days after the large discharge event. Garvine (1991) and Sanders and Garvine (2001) found that velocity fluctuations near the mouth of Delaware Bay lagged discharge measurements at Trenton, NJ by 0–8 days, indicating that increased river discharge would result in increased transport out of the estuary. However, larvae released at the two up-estuary sites (1 and 2) were mostly retained within the bay, due to settlement on the New Jersey shore, which was caused by the strong mixing associated with the large discharge and upwelling winds. Those larvae spawned in mid-summer (July 17) were subjected to upwelling winds and weak discharge, resulting in little settlement and the loss of most larvae from the bay. However the northward transport associated with the upwelling winds did result in some limited settlement of larvae on the New Jersey shore of the bay and greater settlement on the New Jersey shore of coastal ocean.

Overall results of our study showed that the estuarine and coastal circulation typically

found along the Middle Atlantic coast of the United States during the spawning season of *E. sinensis* can result in significant retention of new and established populations in inland bays as well as alongshore transport of larvae to new coastal locations. Examination of the effects of winds, discharge, and likely larval behavior on larval transport in and around Delaware Bay reveals that larvae can settle on both the New Jersey and Delaware shores of the bay and in the adjacent coastal ocean, regardless of initial spawning location, suggesting that *E. sinensis* can easily expand its range. Since little is known about the size or location of the populations of *E. sinensis* in Delaware Bay, results from our study cannot be used to determine the magnitude of larval settlement but do suggest possible locations and timing of settlement. Realistic scenarios indicate comparable settlement along both coasts (Fig. 4), suggesting that sentinel stations be installed along both coastlines to begin monitoring for this invasive species.

Although the rationale for this study was the examination of those physical and biological characteristics that would result in the retention and transport of mitten crabs in Delaware Bay, results from this study are far-ranging. The interactions between physical mechanisms of the flow field and biological characteristics of the larvae can result in drastically different fates for spawned larvae. The modeling approach taken here applies directly to any such species whose larvae undergo common vertical migrations that result in larval retention (Sulkin, 1984). However, our particular study is limited by our lack of knowledge of larval mortality rates, timing of larval release, and spawning location. The different degrees of larval retention due to simulated variations in spawning location and larval behavior underscores the need for a better understanding of the distribution of sedentary adult population to determine larval spawning locations and larval behavior to determine if diel, tidal, or ontogenetic migrations occur under conditions found in Delaware Bay. Future studies should incorporate behavioral experiments to provide appropriate vertical migratory behavior and surveys of the region for planktonic, post-settlement and adult mitten crab populations to validate the coupled numerical model. These studies will have direct implications for mitten crab management, including important aspects of basic larval biology in local estuaries, a mechanistic understanding of the likelihood of establishing large populations in the near future and for the rest of this century, and a more accurate determination of where sentinel stations should be placed for detecting mitten crab settlement.

Acknowledgments. We would like to thank Alan Blumberg for providing the numerical ocean model ECOM3d and Michael Whitney for development of the circulation model. We are also grateful for the comments from two anonymous reviewers. This study was supported by funds from the Delaware Sea Grant College Program and the National Oceanic and Atmospheric Administration. This is contribution number 37 from the Marine Science Center at the University of New England.

REFERENCES

Anger, K. 1991. Effects of temperature and salinity on the larval development of the Chinese mitten crab *Eriocheir sinensis* (Decapoda, Grapsidae). Mar. Ecol. Prog. Ser., *72,* 103–110.

Avicola, G. and P. Huq, 2002. Scaling analysis for the interaction between a buoyant coastal current and the continental shelf: Experiments and observations, J. Phys. Oceanogr., *32,* 3233–3248.

Bax, N., J. T. Carlton, A. Mathews-Amos, R. L. Haedrich, F. G. Howarth, J. E. Purcell, A. Rieser and A. Gray. 2001. The control of biological invasions in the world's oceans. Conserv. Biol., *15,* 1234–1246.

Blanton, J. O., F. E. Werner, A. Kapolnai, B. O. Blanton, D. Knott and E. L. Wenner. 1999, Wind-generated transport of fictitious passive larvae into shallow tidal estuaries. Fish. Oceanogr., *8,* 210–225.

Carlton, J. T. and A. N. Cohen. 2003. Episodic global dispersal in shallow water marine organisms: the case history of the European shore crabs *Carcinus maenas* and *C. aestuarii.* J. Biogeography, *30,* 1809–1820.

Chapman, D. C. 1985. Numerical treatment of cross-shelf open boundaries in a barotropic coastal ocean model. J. Phys. Oceanogr., *15,* 1060–1075.

Chapman, D. C. and S. J. Lentz. 1994. Trapping of a coastal density front by the bottom boundary layer. J. Phys. Oceanogr., *24,* 1464–1478.

Cohen, A. N. and J. T. Carlton. 1995. Biological study. Nonindigenous aquatic species in a United States estuary: a case study of the biological invasions of the San Francisco Bay and Delta. United States Fish and Wildlife Service, Washington, DC and National Sea Grant College Program, Connecticut Sea Grant, NTIS report no. PB96–1666525.

DiBacco, C., D. Sutton and L. McConnico. 2001. Vertical migration behavior and horizontal distribution of brachyuran larvae in a low-inflow estuary: implications for bay-ocean exchange. Mar. Ecol. Prog. Ser., *217,* 191–206.

Dittel, A. I. and C. E. Epifanio. 1982. Seasonal abundance and vertical distribution of crab larvae in Delaware Bay. Estuaries, *5,* 197–202.

—— 2009. Invasion biology of the Chinese mitten crab *Eriochier sinensis:* A brief review. J. Exp. Mar. Biol. Ecol., *374,* 79–92.

Egbert, G. D., A. F, Bennett and M. G. G. Forman. 1994. TOPEX/POSEIDON tides estimated using global inverse model. J. Geophys. Res., *99,* 24821–24852.

Epifanio, C. E. 1995. Transport of blue crab (*Callinectes sapidus*) larvae in the waters off mid-Atlantic states. Bull. Mar. Sci., *57,* 713–725.

—— 2007. Biology of larvae, *in* The Blue Crab *Callinectes sapidus.* V. S. Kennedy and L. E. Cronin, eds., Maryland Sea Grant, College Park, MD, 513–533.

Epifanio, C. E. and R. W. Garvine. 2001. Larval transport on the Atlantic continental shelf of North America: a review. Estuar. Coast. Shelf Sci., *52,* 51–77.

Epifanio, C. E., K. Little and P. M. Rowe. 1988. Dispersal and recruitment of fiddler crab larvae in the Delaware River estuary. Mar. Ecol. Prog. Ser., *43,* 181–188.

Epifanio, C. E., G. Perovich, A. I. Dittel and S. C. Cary. 1999. Development and behavior of megalopa larvae and juveniles of the hydrothermal vent crab *Bythograea thermydron.* Mar. Ecol. Prog. Ser., *185,* 147–154.

Epifanio, C. E. and C. E. Tilburg. 2008. Transport of larval forms near large estuaries of the Middle Atlantic Bight: A wet and windy journey. J. Mar. Res., *66,* 723–749.

Forward, R. B., Jr. 1990. Responses of crustacean larvae to hydrostatic pressure: behavioral basis of high barokinesis. Mar. Fresh. Behav. Phy., *17,* 223–232.

Forward, R. B., H. Diaz and M. B. Ogburn. 2007. The ontogeny of the endogenous rhythm in vertical migration of the blue crab *Callinectes sapidus* at metamorphosis. J. Exp. Mar. Biol. Ecol., *348,* 154–161.

Forward, R. B. Jr. and R. A. Tankersley. 2001. Selective tidal-stream transport of marine animals. Oceanogr. Mar. Biol., *39,* 305–353.

Forward, R. B. Jr., R. A. Tankersley and J. M. Welch. 2003. Selective tidal-stream transport of the blue crab *Callinectes sapidus:* an overview. Bull. Mar. Sci., *72,* 347–365.

Garvine, R. W. 1991. Subtidal frequency estuary-shelf interaction: Observations near Delaware Bay. J. Geophys. Res., *96,* 7049–7064.

Garvine, R. W., C. E. Epifanio, C. C. Epifanio and K. C. Wong. 1997. Transport and recruitment of blue crab larvae: a model with advection and mortality. Estuar. Coast. Shelf Sci., *45,* 99–111.

Garvine, R. W., R. K. McCarthy and K.-C. Wong. 1992. The axial salinity distribution in the Delaware Estuary and its weak response to river discharge. Estuar. Coast. Shelf Sci., *35,* 157–165.

Grosholz, E. D., G. M. Ruiz, C. A. Dean, K. A. Shirley, J. L. Maron and P. G. Connors. 2000. The impacts of a nonindigenous marine predator in a California bay. Ecology, *81,* 1206–1224.

Hannah, C. G., C. E. Naimie, J. W. Loder and F. E. Werner. 1998. Upper-ocean transport mechanisms from the Gulf of Maine to Georges Bank, with implications for *Calanus* supply. Cont. Shelf Res., *17,* 1887–1911.

Hetland, R. D. and W. R. Geyer. 2004. An idealized study of the structure of long, partially mixed estuaries. J. Phys. Oceanogr., *34,* 2677–2691.

Houser, L. T. and C. E. Epifanio. 2009. Impacts of biochemical cues on horizontal swimming behavior of individual crab larvae. Mar. Freshw. Behav. Phy., *42,* 249–264.

Janzen, C. D. and K.-C. Wong. 2002. Wind-forced dynamics at the estuary-shelf interface of a large coastal plain estuary. J. Geophys. Res., *107,* 3138–3150.

Jensen, G. C., P. S. McDonald and D. A. Armstrong. 2002. East meets west: competitive interactions between green crab *Carcinus maenas,* and native and introduced shore crab *Hemigrapsus* spp. Mar. Ecol. Prog. Ser., *225,* 251–262.

Jin, G., Z. Li and P. Xie. 2001. The growth patterns of juvenile and precocious Chinese mitten crabs, *Eriocheir sinensis* (Decapoda, Grapsidae), stocked in freshwater lakes of China. Crustaceana, *74,* 261–273.

Jin, G., P. Xie and Z. J. Li. 2002. The precocious Chinese mitten crab: Changes of gonad, survival rate, and life span in a freshwater lake. J. Crustac. Biol. *22,* 411–415.

Jones, M. B. and C. E. Epifanio. 1995. Settlement of brachyuran megalopae in Delaware Bay: an analysis of time series data. Mar. Ecol. Prog. Ser., *125,* 67–76.

Kim, C. H. and S. G. Hwang. 1995. The complete larval development of the mitten crab *Eriocheir sinensis* H. Milne Edwards, 1853 (Decapoda, Brachyura, Grapsidae) reared in the laboratory and a key to the known zoeae of the Varuninae. Crustaceana, *68,* 793–812.

Kobayashi, S. and S. Matsuura. 1995a. Maturation and oviposition in the Japanese mitten crab *Eriocheir japonicus* (De Haan) in relation to their downstream migration. Fisheries Science, *61,* 766–775.

—— 1995b. Reproductive ecology of the Japanese mitten crab *Eriocheir japonicus* (De Haan) in its marine phase. Benthos Res., *49,* 15–28.

Kourafalou, V. H., T. N. Lee, L.-Y. Oey and J. D. Wang. 1996. The fate of river discharge on the continental shelf. 2. Transport of coastal low-salinity waters under realistic wind and tidal forcing. J. Geophys. Res., *101,* 3435–3455.

Lodge, D. M., S. Williams, H. J. MacIsaac, K. R. Hayes, B. Leung, S. Reichard, R. N. Mack, P. B. Moyle, M. Smith, D. A. Andow, J. T. Carlton and A. McMichael. 2006. Biological invasions: recommendations for US policy and management. Ecol. Appl., *16,* 2035–2054.

Lohrer, A. M. and R. B. Whitlatch. 2002. Relative impacts of two exotic brachyuran species on blue mussel populations in Long Island Sound. Mar. Ecol. Prog. Ser., *227,* 135–144.

Luckenbach, M. W. and R. J. Orth. 1992. Swimming velocities and behavior of blue crab (*Callinectes sapidus*) megalopae in still and flowing water. Estuaries, *15,* 186–192.

MacDonald, J. A., R. Roudez, T. Glover and J. S. Weis. 2007. The invasive green crab and Japanese

shore crab: behavioral interactions with a native crab species, the blue crab. Biol. Invasions, *9,* 837–848.

Montu, M., K. Anger and C. deBakker. 1996. Larval development of the Chinese mitten crab *Eriocheir sinensis* H. Milne-Edwards (Decapoda: Grapsidae) reared in the laboratory. Helgolander Meeresun., *50,* 223–252.

Münchow A. and R. W. Garvine. 1993. Buoyancy and wind forcing of a coastal current. J. Mar. Res., *51,* 298–322.

Najjar, R. G., C. R. Pyke, M. B. Adams, D. Breitburg, C. Hershner, M. Kemp, R. Howarth, M. R. Mulholland, M. Paolisso, D. Secor, K. Sellner, D. Wardrop and R. Wood. 2010. Potential climate-change impacts on the Chesapeake Bay. Estuar. Coast. Shelf Sci., *86,* 1–20.

Natunewicz, C. C., R. W. Garvine and C. E. Epifanio. 2001. Transport of crab larvae patches in the coastal ocean. Mar. Ecol. Prog. Ser. *222,* 143–154.

Olmi, E. J. 1995. Ingress of blue crab megalopae in the York River, Virginia, 1987–1989. Bull. Mar. Sci., *57,* 753–780.

Panning, A. 1939. The Chinese mitten crab. Annu. Report Smithsonian Inst., 1938, 361–375.

Petrone, C. J., L. B. Jancaitis, M. B. Jones, C. C. Natunewicz, C. E. Tilburg and C. E. Epifanio. 2005. Dynamics of larval patches: spatial distribution of fiddler crab larvae in Delaware Bay and adjacent waters. Mar. Ecol. Prog. Ser., *293,* 177–190.

Pimentel, D., L. Lach, R. Zuniga and D. Morrison. 2000. Environmental and economic costs of nonindigenous species in the United States. Bioscience, *50,* 53–65.

Rudnick, D. A., K. M. Halat and V. H. Resh. 2000. Distribution, ecology and potential impacts of the Chinese mitten crab (*Eriocheir sinensis*) in San Francisco Bay. University of California, Berkeley, Water Resources Center, Contribution 26, 74 pp. www.waterresources.ucr.edu.

Rudnick, D. A., K. Hieb, K. F. Grimmer and V. H. Resh. 2003. Patterns and processes of biological invasion: The Chinese mitten crab in San Francisco Bay. Basic Appl. Ecol., *4,* 249–262.

Ruiz, G. M., L. Fegley, P. Fofonoff, Y. Cheng and R. Lemaitre. 2006. First records of *Eriocheir sinensis* H. Milne Edwards, 1853 (Crustacea:Brachyura: Varunidae) for Chesapeake Bay and the mid-Atlantic coast of North America. Aquatic Invasions, *1,* 137–142.

Ruiz, G. M., P. W. Fofonoff, J. T. Carlton, M. J. Wonham and A. H. Hines. 2000. Invasion of coastal marine communities in North America: apparent patterns, processes, and biases. Annu. Rev. Ecol. Syst., *31,* 481–531.

Sanders, T. M. and R. W. Garvine. 2001. Fresh water delivery to the continental shelf and subsequent mixing: an observational study. J. Geophys. Res., *106,* 27087–27101.

Smagorinsky, J. 1963. General circulation experiments with the primitive equations, 1. The basic experiment. Mon. Weather Rev., *91,* 99–164.

Smolarkiewicz, P. K. and W. W. Grabowski. 1990. The multidimensional positive definite advection transport algorithm, J. Comput. Phys., *86,* 355–375.

Sorte, C. J. B., S. L. Williams and J. T. Carlton. 2010. Marine range shifts and species introductions: comparative spread rates and community impacts. Global Ecol. Biogeogr., *19,* 303–316.

Sulkin, S. D. 1984. Behavioral basis of depth regulation in the larvae of brachyuran crabs. Mar. Ecol. Prog. Ser., *15,* 181–205.

Tilburg, C., A. I. Dittel and C. E. Epifanio. 2007a. Retention of crab larvae in a coastal null zone. Estuar. Coast. Shelf Sci., *67,* 570–578.

—— 2009. High concentrations of crab larvae along the offshore edge of a coastal current: Effects of convergent circulation. Fish. Oceanogr., *18,* 135–146.

Tilburg, C. E., R. W. Houghton and R. W. Garvine 2007b. The mixing of a dye tracer in the Delaware plume: Comparison of observations and simulations. J. Geophys. Res., *112,* Art. No. C12004.

Tilburg, C., L. T. Houser, C. N. Steppe, R. W. Garvine and C. E. Epifanio. 2006. Effects of coastal transport on larval patches: Models and observations. Estuar. Coast. Shelf Sci., *67,* 145–160.

Tilburg, C. E., J. T. Reager and M. M. Whitney. 2005. The physics of blue crab larval recruitment in Delaware Bay: A model study. J. Mar. Res., *63,* 471–495.

Tilburg, C. E., J. Seay, T. D. Bishop, H. L. Miller III and C. Meile. 2010. Distribution and retention of *Petrolisthes armatus* in a coastal plain estuary: the role of vertical movement in larval transport. Estuar. Coast. Shelf Sci., *88,* 260–266.

Veldhuizen, T. 1998. What difference can one crab species make? The ongoing tale of the Chinese mitten crab and the San Francisco Estuary. Outdoor California, *59,* 19–21.

Visser, A. W. 1997. Using random walk models to simulate the vertical distribution of particles in a turbulent water column. Mar. Ecol. Prog. Ser., *158,* 275–281.

Whitney, M. M. and R. W. Garvine. 2006. Simulating the Delaware Bay buoyant outflow: Comparison with observations. J. Phys. Oceanogr., *36,* 3–21.

Williams, A. B. 1984. Shrimps, Lobsters, and Crabs of the Atlantic Coast of the Eastern United States, Maine to Florida. Smithsonian Institution Press, Washington, DC, 550 pp.

Wong, K. C. and A. Münchow. 1995 Buoyancy-forced interaction between the estuary and inner shelf: observation. Cont. Shelf Res., *15,* 59–88.

Xia, M., L. Xie and L. J. Pietrafasa. 2007. Modeling of the Cape Fear River estuary plume. Estuar. Coast., *30,* 698–709.

Yankovsky, A. E. and D. C. Chapman. 1997. A simple theory for the fate of buoyant discharges. J. Phys. Oceanogr., *27,* 1386–1401.

Zhang, T. L., Z. J. Li and Y. B. Cui. 2001. Survival, growth, sex ratio, and maturity of the Chinese mitten crab (*Eriocheir sinensis*) reared in a Chinese pond. J. Freshwater Ecol., *16,* 633–640.

Zhao, N. 1980. Experiments on the artificial propagation of the woolly-handed crab (*Eriocheir sinensis* H. Milne-Edwards) in artificial sea water. J. Fish. China, *4,* 95–104.

Received: *3 February, 2011;* revised: *9 June, 2011.*